

VSS-T

National Aeronautics and Space Administration  
Goddard Space Flight Center  
Contract No. NAS-5-12487

ST- LPS- LS- 10722

FACILITY FORM 602

N 68-25742	
(ACCESSION NUMBER)	
19	(THRU)
(PAGES)	
02-94918	(CODE) 30
(NASA CR OR TMX OR AD NUMBER)	(CATEGORY)

ON THE NATURE OF LIGHT RAYS ON THE MOON

by

Yu. N. Lipskiy &  
V. V. Shevchenko

GPO PRICE \$ \_\_\_\_\_

(USSR)

CFSTI PRICE(S) \$ \_\_\_\_\_

Hard copy (HC) 306

Microfiche (MF) \_\_\_\_\_

ff 653 July 65



5 JUNE 1968

ON THE NATURE OF LIGHT RAYS ON THE MOON

(\*)

Astronomicheskii Zhurnal,  
Tom 45, No.2, 389 - 398,  
Izd-vo "NAUKA", 1968

by Yu. N. Lipskiy  
& V. V. Shevchenko

SUMMARY

Comparison of ground observation data with the results of photographing the lunar surface by spacecrafts leads to the conclusion that the structural peculiarity of light rays is the increased concentration of craters with diameter of 800 - 200 m. A comparative photometric analysis of parts of rays allows us to elicit the availability of meso-shady function generated by craters of a given size, and thus, to extrapolate the well known structural properties of the mentioned morphological category.

\*  
\* \*

The earlier widely propagated representation on light rays as formations of poured character, constituting a thin layer of clear substance [1, 2], is currently subject to radical revision. The traditional viewpoint concerning the nature of light rays was based upon a series of characteristic peculiarities of these formations. Among them one may point to a relatively sharp increase of brightness at fullmoon time, the invariability of direction and contour of separate rays at their crossing of morphologically distinct regions, the absence of any kind of signs of disruption of the relief shape during their intersection by rays, and the total absence of relief signs even in the direct vicinity of the terminator.

However, the peculiar course of brightness variation with phase was noted long ago; it was expressed in that the contrast of rays and of the surrounding surface rises sharply with the approaching of fullmoon, while it drops rapidly as this phase recesses. The curves of brightness variation of radial systems prior and after fullmoon are often asymmetrical. The given peculiarities have constituted at observations made from Earth, the first and most significant signs of the fact that the representations of light rays as being a thin layer of a substance of increased luminosity do not fully exhaust the available observation material.

---

(\*) O PRIRODE SVETLYKH LUCHEY NA LUNE

1. Photographs of the lunar surface from close distance and gradual increase of image resolution from a few kilometers to fractions of meter have shown the separation of initially uniform clear spots into discrete light points having proved to be, after a still more detailed consideration, separate craters.

According to the results of analysis of RANGER-7 photographs, conducted at the JPL in Pasadena, USA [3], Tycho crater-originating light ray area has such a structure, the latter being situated within Mare "Poznannc" [transliteration]. Moreover, authors of the State Astronomical Institute of Shternberg (GAISH), studying Ranger-7's camera A photos, have traced the form variation of nearly 30 areas which look on photographs taken from Earth under analogous illumination conditions as regions of increase brightness, that is of sufficiently uniform light spots (Fig.2). This resulted in the corroboration of the fact that all the regions examined, to the extent permitted by resolution of Ranger-7 photographs, have a structure analogous to that shown in Fig.1. Some of quantitative

T A B L E 1

Number of Region	Number of craters distinguishable on the photo	Dimension in met. of largest crat.	Average crater dimension in m,	Mean value of distances between craters, m.
1	30	650	300	900
2	8	650	400	900
3	10	1200	300	850
4	3	1450	500	500
5	100	800	200	100
6	30	1250	300	700
7	50	800	300	500
8	15	700	300	900
9	10	1300	500	1000
10	10	1100	400	500
11	10	1500	400	1000
12	10	600	300	1000
13	10	1200	600	800
14	10	1000	400	800
15	15	1200	500	900
16	10	1200	400	800
17	5	800	300	300
18	10	900	400	700
19	10	1200	300	900
20	20	800	200	400
21	50	800	200	400
22	5	1000	300	400
23	5	800	200	400
24	4	700	200	300
25	10	800	200	300
26	5	1000	400	800
27	5	1000	300	700
28	15	600	200	600
29	30	800	200	600

characteristics obtained at that time are shown in Table 1, where the numbers of the regions are given in column 1 in accord with Fig.2, the remaining columns giving the measurement data after the photos of RANGER-7. It should be taken into account that, according to [4], the limit diameters that lend themselves to resolution on the Fig.2 photos are of 1.4 km.

Particular interest is offered also by the distribution of craters by the size of the areas related to the light ray. An analogous calculation was conducted for region No.5 according to the A-196 photograph of RANGER-7, having a scale of 1 mm to 45 m, for which the least distinguishable craters reached about 80 m in diameter. The area bounded by the contours of the clear portion of region No.5, constituted according to Fig.2, 65 km<sup>2</sup>. The results obtained are compiled in Table 2, column 1.

Presented in column II of the same

T A B L E 2

Table 2 are the data according to general statistics of craters in Mare Poznan-nom [Russian] converted to

Size of craters, in m.	I	II
800 - 400	16	2
400 - 200	38	32
200 - 100	35	65
100 - 80	14	200

65 km<sup>2</sup>. Obviously, the sharp redistribution of the number of craters in the region of the light ray is striking by comparison with the averaged data along the whole

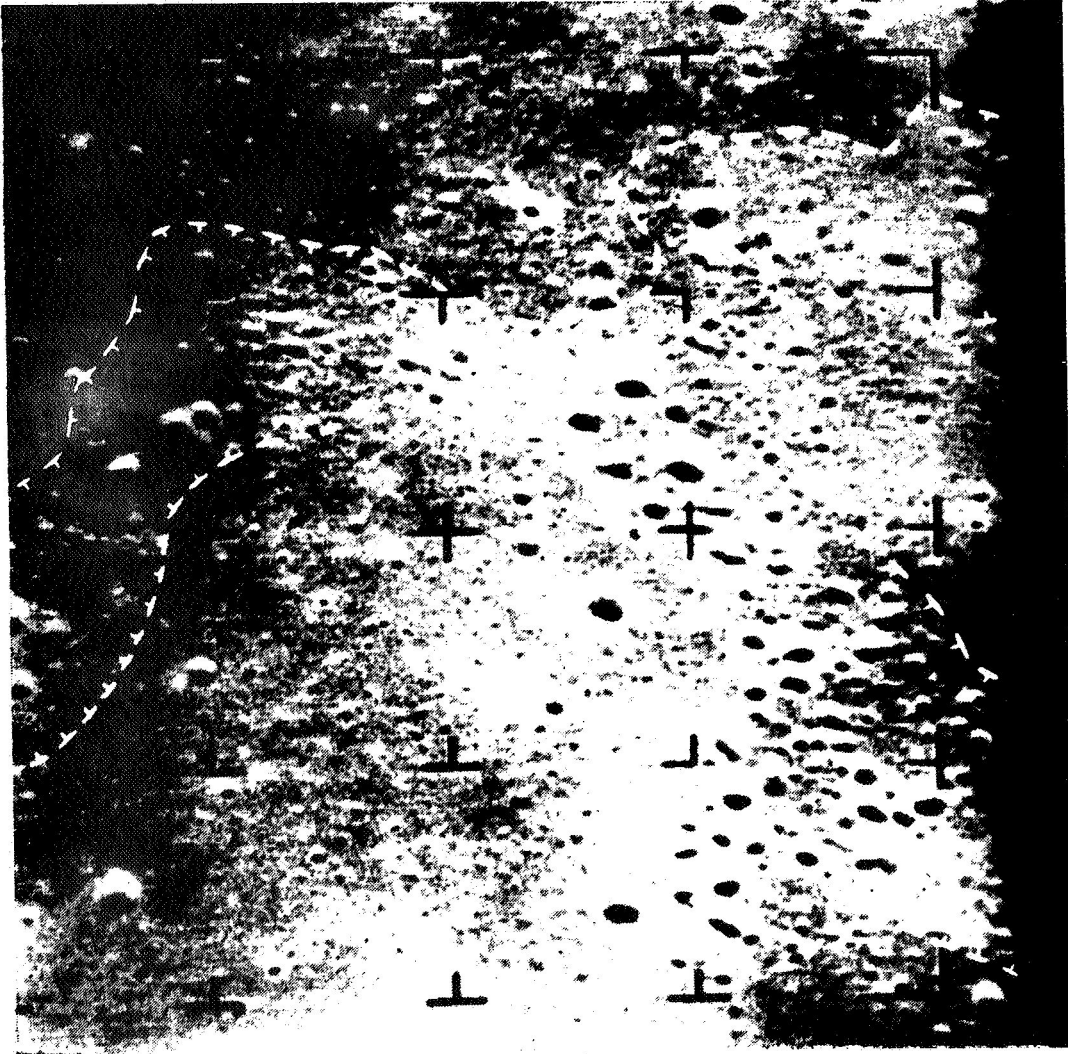


Fig.1. Photo A-196 obtained by RANGER-7. The boundary  
is shown of a part of the ray from crater Tycho, which  
has a character of a light spot in photographs with less  
resolution



Fig.2. Part of the sheet E5-c from reference [19]  
with boundaries of investigated spots

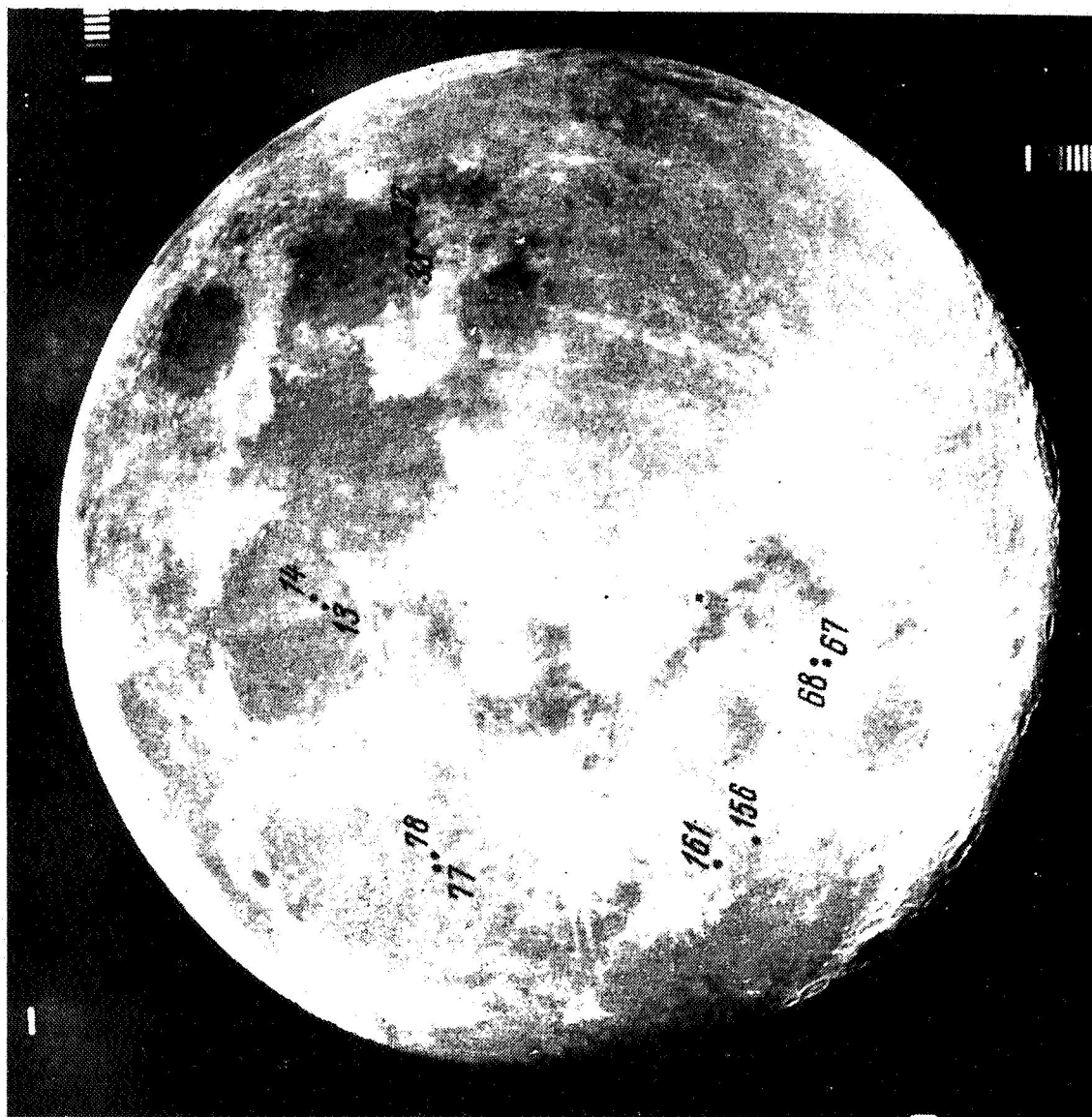


Fig.3. Position of the portions of visible hemisphere whose results of measurements are shown in Figure 4.

surveyed region toward the side of substantial prevalence of large craters and those of medium size. Comparison of these data points to the decisive significance of increased concentration of relatively large craters (800 to 200 m in diameter) for the form of the area considered with a resolution attainable by terrestrial observations.

2. It was recalled above that the most significant sign of structural peculiarities of light rays observed from Earth is the character of phase variation of brightness.

Let us now turn to the results of photometric investigations. The indicated photometric properties are reflected in numerous catalogs including the results of measurements of brightness variations of rays during lunation time. Let us pause at the comparative characteristic of brightness variation of light rays and portions of maria adjacent to them measured by Fedorets [5]. Data on twelve selected twin areas show that during fullmoon time contrast between the ray and the surrounding surface reaches a maximum, while for greater phase values it drops to zero.

Under conditions of ground observations it is particularly important to trace the brightness variation as a function of the angle of light incidence, inasmuch as for a given formation the latter remains practically invariable. With this in view five areas of light rays with the corresponding five neighboring areas were chosen from the catalog [5], for comparison in different parts of the visible hemisphere (see Fig.3). The identification of clear regions with concrete radial systems were conducted by the radial systems' map of the visible hemisphere [6] having a scale 1: 3,800,000. The data indicated are plotted in the form of curves in Figures 4 a, b, c, d, e. — Area No.13 (the number of areas corresponds to the order adopted in the catalog [5]) is related to crater "Menelay" and Mare Serenitatis; No.17 is a comparison area; No.32 is an area in Mare Foecunditatis, at the intersection of craters Tycho, Stevinus and Langren; No.33 is a comparison area; No.67 is an area of crater Tycho's ray, which is located in the Mare Nubium; No.68 is a comparison area; No.77 is the ray area of Copernicus crater which is in the Mare Imbrium; No.78 is a comparison area; No.161 is an area of Kepler crater's ray, which is in the Oceanus Procellarum; No.156 is a comparison area.

The curves of Fig.4 (next page) show that for fullmoon and local noon, the contrast between the areas of rays and those of comparison is rather substantial. However, despite the unquestionable difference in albedo, their brightness for a low altitude of the Sun above local horizon is smoothed out with an error to the precision of measurements. Such a peculiarity leads to the natural conclusion about the structural difference of area of rays and comparison mare areas. The same conclusion was arrived at by Fedorets [5] on the basis of a more rapid brightness increase of clear rays with respect to the surface surrounding them.

The fact that the comparative characteristic of the reflectivity of rays remains independent of the location of the measured areas on the visible hemisphere of the Moon speaks of unquestionability of general properties of rays as a morphological category of lunar formations.

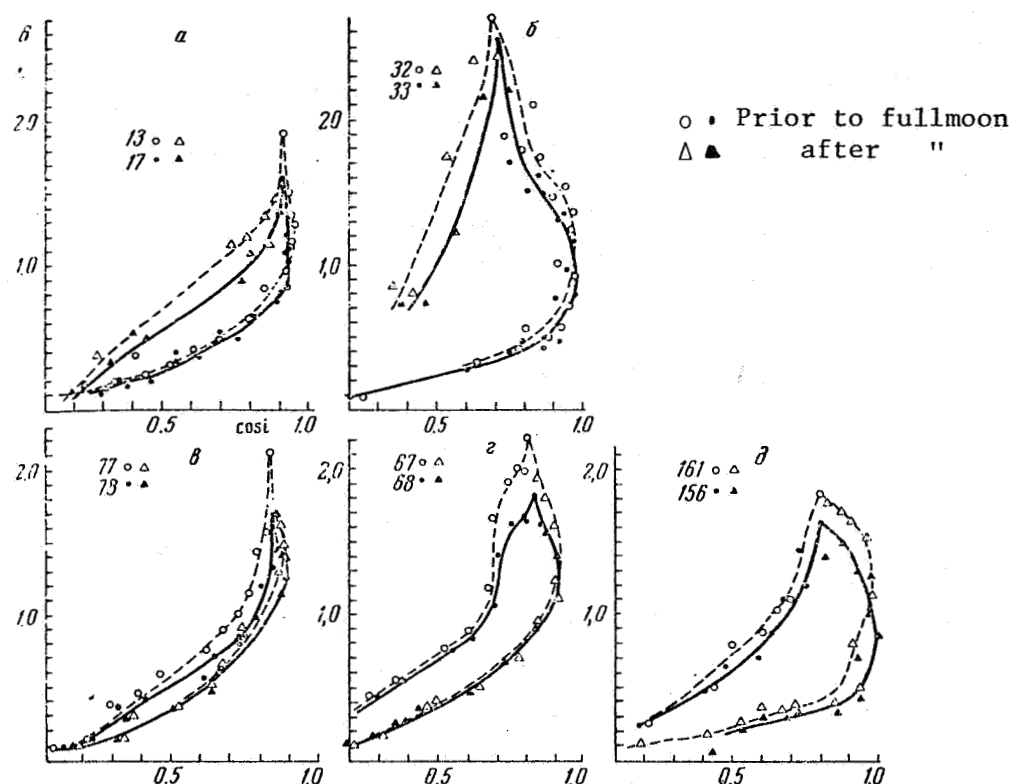


Fig.4. The brightness is plotted in ordinates in relative units and the cosine of incident angle is plotted in abscissa

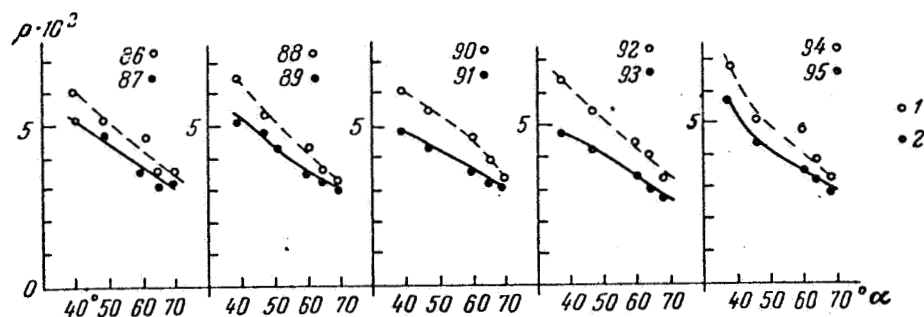


Fig.5. 1 denotes the values of brightness of light rays and 2 denotes the values of brightness of comparison areas

This position becomes still more evident owing to the investigations of the far side of the Moon, which, as is well known, has substantial microrelief differences [7]. In connection with this it is interesting to bring forth the results of photometric investigations of rays of crater Numerov ( $\lambda = -114^\circ$ ,  $\beta = +21^\circ$ ) based upon the photographing material of lunar surface by AIS ZOND-3 in 1965. In Fig.5 we plotted the curves of comparative variation of brightness expressed by the brightness factor  $\rho$  of rays and adjacent areas of comparison



as a function of the value of phase angle. The curves are plotted according to data of the "Catalog of Photometric Characteristics of Selected Objects of Far Side's Eastern Sector" [8]. A specific expression of contrast variation is noted in a small available interval of  $\alpha$  variation. The data brought up are related to the eastern branch of the radial system, reminding by its shape the system of Proclus crater on the visible side of the Moon. With the view of increasing the interval variation of angular parameters and of the number of measured areas (Fig.6) we conducted additional measurements involving some of the photographs of AIS "ZOND-3", transmitted in conditions of rapid reviewing (see [8]). The method of processing these images amounted to the following.

A series of points from the Catalog of photometric characteristics.. (Fig.7) was identified on the photograph by general configurations of large-scale formations and reviewing of oscillographic recordings of the respective lines. From the phase curves constructed according to the "Catalog" we took down the brightness of each point at a phase value corresponding to the photograph processed. The thus obtained calibration curve of the photograph fixes the correspondence between the amplitude of oscillographic recordings and the brightness factor (Fig.8). By way of consequence, we obtain the photometric tying of measurements in the "Catalog"'s absolute system.

The geometric tying was conducted by graphic method, whereupon the same points served as a basis, of which the selenographic coordinates are known with sufficient precision for photometric measurements [8]. Upon determination of the position on the photograph of the center of projection and the direction of the central meridian, subsequent measurements were conducted in the polar system of coordinates: radius-vector  $\rho_B$  and azimuth  $\alpha_B$ . The selenographic coordinates of the investigated points were reconverted into polar coordinates and the needed point was plotted on the unfolded complete cadre of photos' sketching board. According to these data we measured the corresponding amplitude on the oscillograph recording. Nine cadres were processed in all in conditions of rapid reviewing. Because of the fact that the discrete structure of the cadre does not assure the possibility of measurement of brightness of one and the same point, of the area on all cadres, only the data according to photographs in which the measured areas were reliably identified were entered in the final results.

One of the characteristic peculiarity of photographing conditions of lunar surface by AIS "ZOND-3" was the invariability of light incidence angle (the entire photographing session lasted only about one hour) with the variation of the phase angle within a rather broad interval. For the portions of surface in the region of crater Numerov's radial system the variations of reflection angles were also found to be insignificant. As the phase increased, the azimuth between the planes of incident and reflected rays varied substantially. This parameter was precisely chosen as the "determinant" for the analysis of the results obtained. Plotted in Fig.9, a - e the curves of the course of brightness expressed by the brightness factor  $\rho$  for ray and neighboring areas of comparison of continual areas. Analysis of these curves shows the presence of the aforementioned effect of contrast variation between rays and the surface surrounding them.

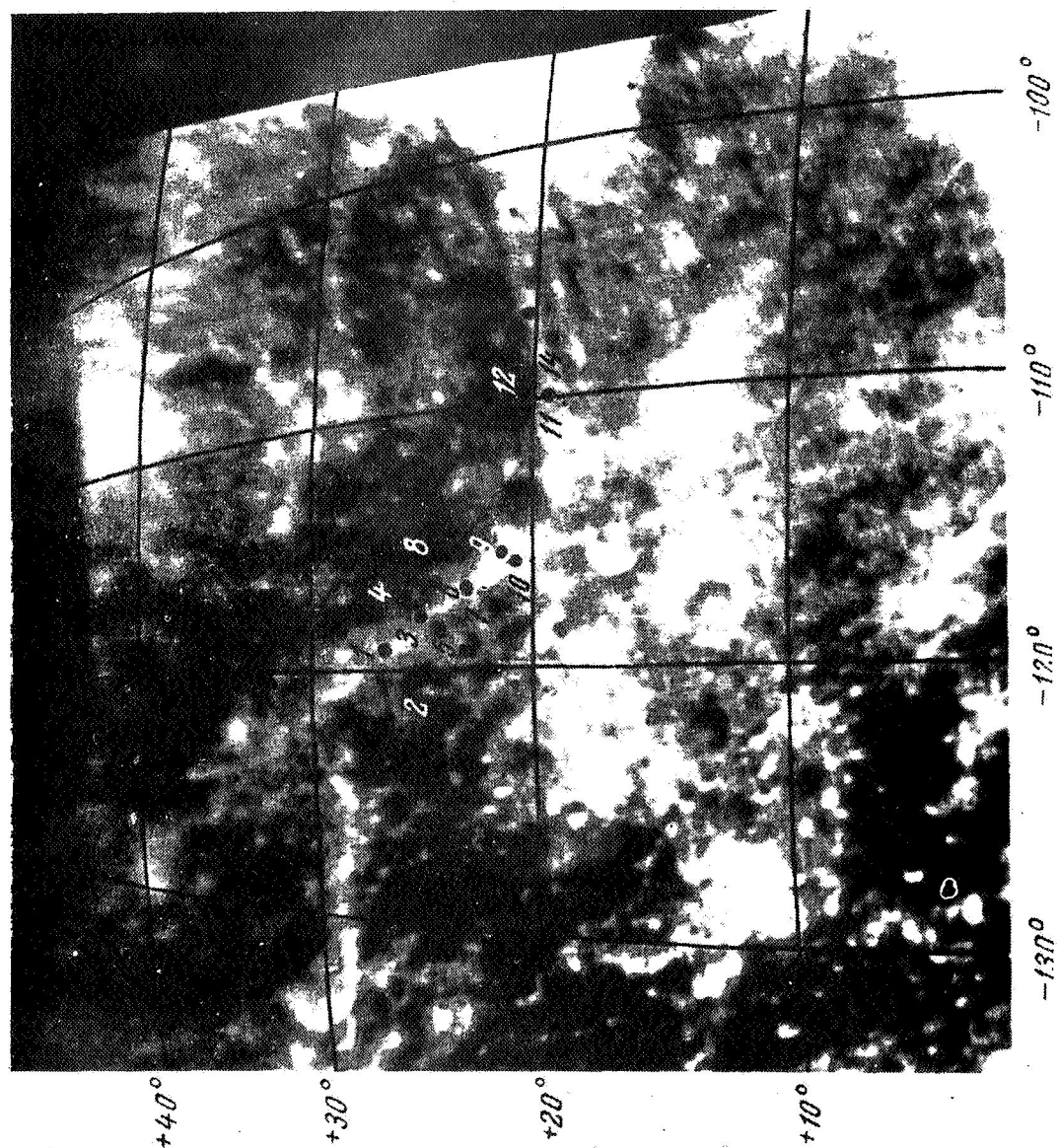


Fig. 6. Reprojection on a sphere of part of one of the photographs obtained on AIS "ZOND-3" with indicated points of measured areas. The reprojection was made in the Physics of the Moon Division of the Shternberg State Astronomical Institute (GAISH). The North is above

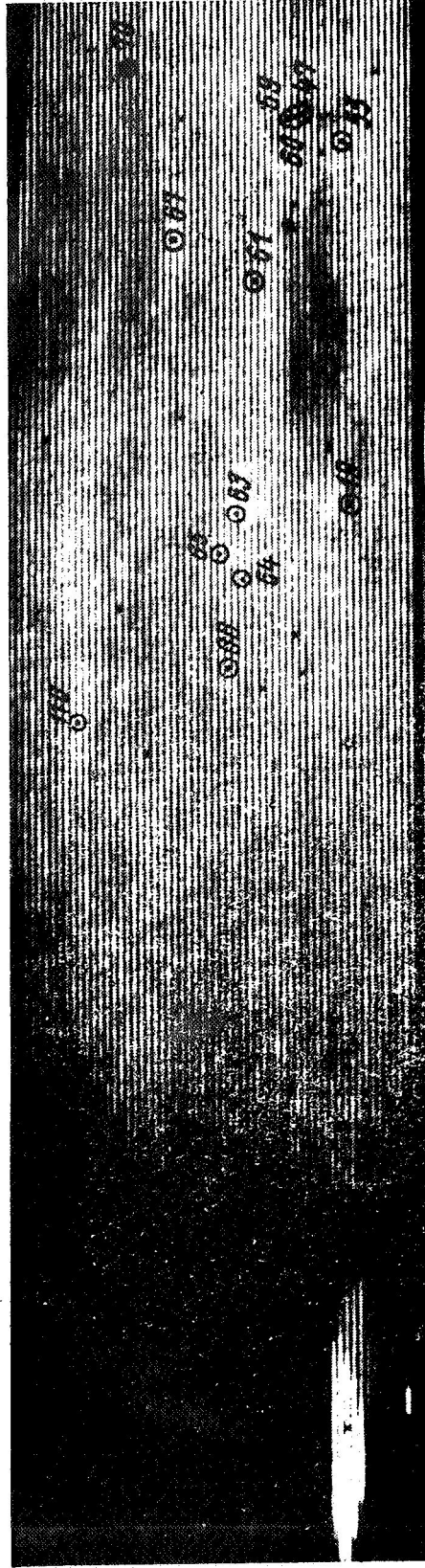


Fig.7. Photograph No.15 from the series of photos obtained by AIS "ZOND-3"  
transmitted in rapid reviewing regime

3. It appears to be of great importance also to examine certain calorimetric peculiarities of radial systems.

Investigations by visual and photovisual ways in a relatively narrow wavelength interval (380 - 560 $\mu$ ) [9] show no substantial variations in the color of rays, as well as of the entire lunar surface. However, the widening of the indicated interval leads to significant results. Measurements conducted by Barabashev and Chekirda [10] and in the portions of spectra 840, 650, 502, 415 and 365 of rays of Tycho, Copernicus and Kepler craters, provided information on color variation along separate branches of radial systems; at the same time, at a known range from system's center, the obtained ray color indicator does not correspond to the analogous characteristic of the basic crater. This fundamental conclusion is still further corroborated by recent investigations by J. Adams (JPL, USA). He obtained by means of the 30 inch reflector of the Stone Ridge Observatory photographs of the Moon 3.8 days after fullmoon with three filters having maxima near 390, 510, 750 m $\mu$ . The kinds of photofilms were assorted according to the characteristics of light-filter. A combined color print with exaggerated color separation was obtained from three black-and white negatives. According to the analysis carried out [11], the color of rays (of Kepler crater in particular) varies correspondingly with the color of the surface intersected by them. The conclusion of color reception by rays corresponding to the surrounding surface is confirmed by a series of other authors' research too. Thus, the two-color photograph, obtained by Whitaker [12], using the "sandwich" method, i. e. adding the negative of one photograph with the positive of the other, provides a visual representation of the aforementioned property. The same photograph of the region of radial systems of craters Aristarchus, Kepler and Copernicus was obtained at GAISH (State Astronomical Institute of Shternberg). To compose it two negatives of full Moon, respectively exposed through light-filters UFS-6 (maximum near 350 m $\mu$ ) and KC-14 (720 $\mu$ ). This photograph shows that in the light-separation image the branching structure of radial systems nearly vanishes and the separate rays at the background of the surrounding surface are extremely weakly outlined or are lost altogether, assuming the color of the underlying layer (Fig.10).

4. Attempts to explain the character of lunar photometric function and, in particular of the singularities of ray reflectivity, by way of combinations at the given moment of time of visible, illuminated and shadowed parts inside separate craterlets, were also made earlier. However, the nondifferential approach and the striving of creating a unique model for morphologically specifically diversified formations on the Moon have led to some scholastic shapes of the relief, for example, semiellipsoidal craterlets with depth exceeding the radius 2.5 to 3 times [13]. In the final resort all such models reflected only the most general characteristic of the lunar surface, i. e., its "furrowed" state.

The assumption that alongside with increased albedo the light rays have a higher order "digging" than the surface surrounding them, was suggested in its time by Barabashev [14] when analyzing the photometric properties of radial systems.

Let us clarify to what extent the structural model of the portions of rays considered in section 1 satisfies the observed characteristics of these formations. Let us turn to the static picture of clear rays' visibility in phases

close to fullmoon. According to the subdivision of epochs of relief formation by Khabakov [15], the formation of radial systems is referred to the newest or Copernicus period. Secondary ray craters are the youngest formations of the lunar surface. This explains their "superimposition" to older structures, and also the increased brightness of the internal surface of craterlets. The last case stems from the effect of Moon's surface layer darkening as a result of prolonged action of the solar wind. This effect is also corroborated by some laboratory experiments [16]. It is in order to assume that the relatively fresh erosion of surface matter has a higher albedo. The very same model corresponds to the phenomenon of reception by rays of the color characteristic of the underlying soil.

Further, using the example of instruments presently applied for photographing the Moon with high resolution [4], let us consider the possibilities of making apparent the structure of rays, utilizing the ground observations.

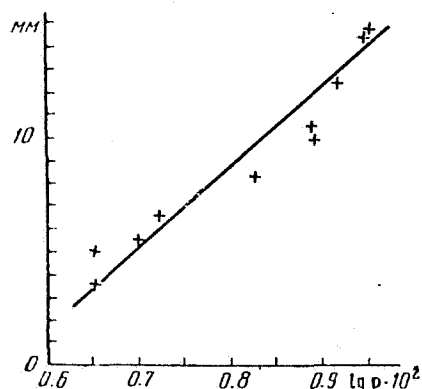


Fig.8. Calibrated curve for the photograph No.15. The values of amplitudes of oscillographic recordings are plotted in the abscissa in mm

The values of diameters of objectives  $D$ , the corresponding them values of diffraction disk  $\alpha_r$ , the radius in angular measure (without taking into account the turbulent motion in the atmosphere) [17] and the linear magnitude of that radius  $r$  in projection on the lunar surface, are compiled in Table 3.

Turning back to the data of Table 1, we find that, basically, the secondary ray craters have dimensions smaller or equal to the diameter of the diffraction disk. Consequently, in a phase close to fullmoon, each craterlet may be viewed as a point source of substantial brightness

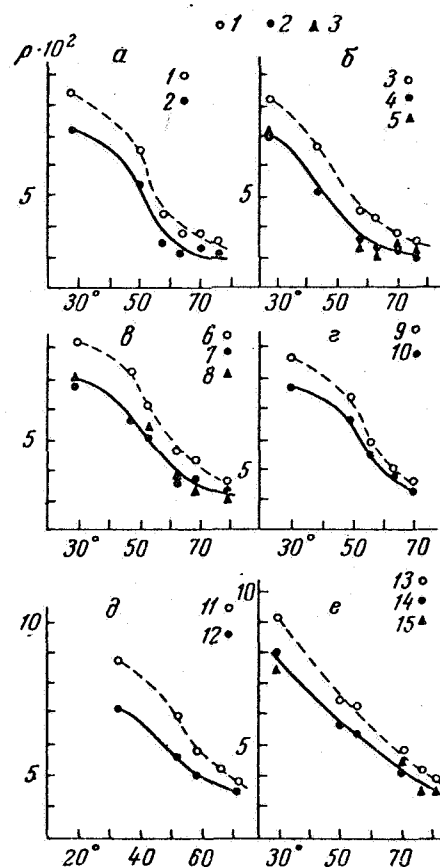


Fig.9. 1) values of brightness of light rays; 2), 3) brightness of comparison areas

TABLE 3

Observatory	$D, \text{mm}$	$\alpha_r$	$r, \text{m}$
Pic du Midi (France)	1060	0.13"	250
Kottamia (UAR)	1870	0.08	160
Hayderabad (India)		0.12	230



Fig.10. Part of the combined photograph.  
composed from negatives obtained in UV  
and infrared by means of a 70-cm reflector  
of the State Astronom. Institute. Shternberg

According to absolute photometric measurements by Sytinskaya [18], the brightness factor  $\rho$  constitutes for rays 0.131 as an average. One should, however, take into account that each elementary craterlet has a lesser brightness. Data of Table 1 show that the distances between craters get closer to the values corresponding to the diameter of the diffraction disk. But these values are overrated, inasmuch as all the investigated areas disappeared from the camera's visual field before a resolution in all details. Region No.5 whose data are the most exhaustive, does constitute an exception. In this case the distances between the geometrical centers of point objects are less than the radius of the diffraction disk. Then, separate objects do not lend themselves to resolution and we observe their combined brightness. The picture of comparatively uniform light bands, observed in ground telescopes and from near-lunar distances for an insufficient resolution of the optical system, is reproduced in the same way, (ref. to [19]).

Let us now pass to the consideration of the dynamic pattern. If we express the area of the image in units of area of the diffraction disk, and that of the glowing element on the Moon is taken as not emerging beyond the limits of diffraction disk's projection on the lunar surface, then, postulating that the brightness variation  $B$  of the area as a function of angular parameters takes place according to a certain function  $F(\epsilon, i, a)$ , we shall obtain

$$E = kB_0 f(\epsilon, i, a) \sigma,$$

where  $E$  is the illumination in the focal plane of the telescope and  $k$  is a constant factor.

The illuminated area  $\sigma$  is also a certain function  $\phi(\Sigma)$  that may be considered as an expression of the shadow function. Then, according to the adopted structural model, function  $\phi(\Sigma)$  for an element of ray has a greater steepness than the analogous function for an element of the comparison area. This peculiarity is explained by the fact that in the latter case, a mesoshadow function is superimposed to a microshadow function, identical for the comparison area and for the inner surface of craterlets, in the scale of a separate craterlet.

Let us conduct analysis of photometric curves brought out in section 2, so as to ascertain the signs of the indicated mesoshadow function.

On the photograph A-196 of RANGER-7 shadow shapes and dimensions were measured for nearly 60 craters with diameter from 400 to 900 meters. It was established that the shape of craterlets may be modeled by a spherical segment; at the same time the craterlet's depth  $h$  ratio to diameter  $d$  fluctuated from 0.15 to 0.25.

Shown in Fig.11 (next page) are the curves of variations in the difference of ray brightness and of comparison areas with the variation of light incidence angle. The curves are plotted on the basis of graphs from Fig.4.

For the data of craterlet geometric characteristics, the angle of the inner slope relative to horizontal plane, conditionally drawn along the cut of crater

edges, is determined by the formula

$$\operatorname{tg} \frac{\xi}{2} = 2 \frac{h}{d}.$$

Then the value of angle  $i$ , for which there appears or disappears a shadow inside the craterlet, i. e., corresponding to the beginning and the end of manifestation if the mesoshadow function, will be called critical. It is equal to  $i_{cr} = 90^\circ - \xi$ . For the craters measured we have  $\xi = 34 - 53^\circ$  and  $i_{cr} = 56 - 37^\circ$

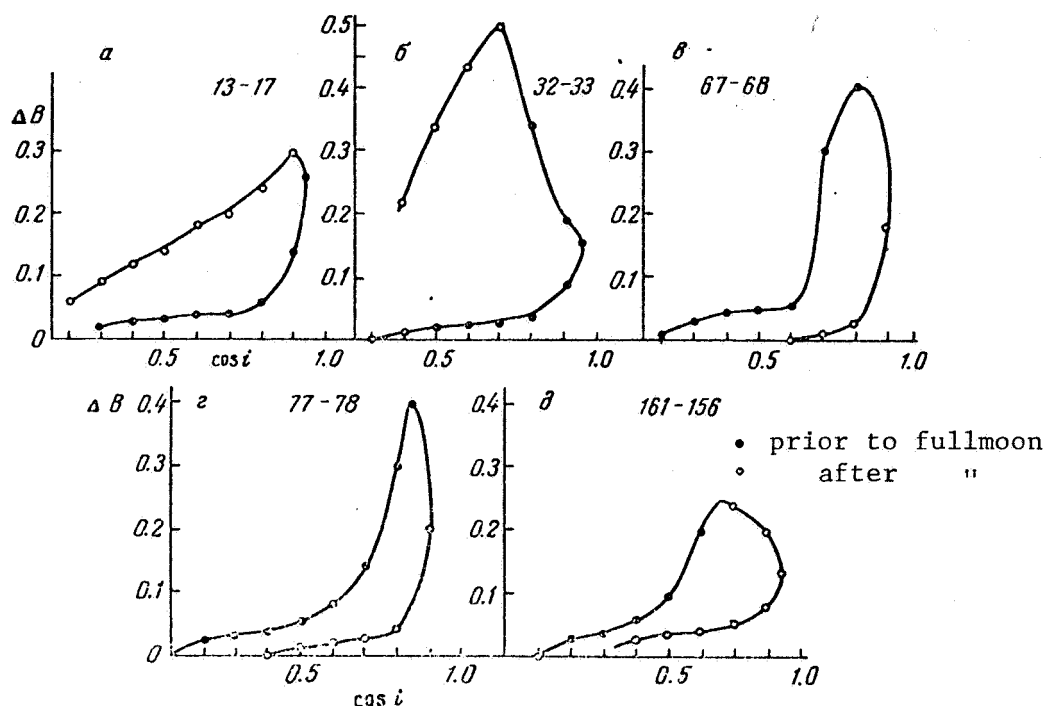


Fig.11. Curves of difference variation in brightness of the ray and of comparison area

Turning to Fig.11, we reveal the inflection of the function at the value  $\cos i = 0.6 - 0.8$ , which corresponds to  $i_{cr}$  ( $a, b$  prior to fullmoon,  $g, z, d$  after fullmoon). Moreover, the general course of curves in Fig.11 can also be explained by the presence of the mesoshadow function. Let us analyze in detail the variation of brightness of a portion of the ray for the cases  $\sigma$  and  $\partial$ . Both these areas lie near the lunar equator, but on both sides of the central meridian. Most clearly expressed discrepancy of two curves is the fact that the brightness difference of areas compared, located to the east of the central meridian, is greater after fullmoon than prior to it for the same values of  $i$ . The opposite is observed for western areas.

Let us consider the process of brightness variation and brightness difference on the example of a solitary craterlet, taking account of the fact that the total brightness of the ray is determined by the combination of brightnesses of elementary craterlets.



In the case  $\sigma$  the invisible part of the inner surface of the craterlet is disposed from the west (Fig.11, a and 11, $\sigma$ ). As the height of the Sun varies the shadow retreats from west to east (Fig.12,a). This is illustrated by the hollow part of the curve in Fig. 11, $\sigma$ . After the passage of the angle value  $i_{cr}$ , the shadow disappears inside the craterlet, to which corresponds an abrupt increase of crater's brightness (manifestation of increased albedo) and the simultaneous rise in the difference of brightnesses of the ray and comparison area. After fullmoon, for the value  $i_{cr}$ , the shadow appeared at the western edge of the craterlet (Fig.12, ), but this did not reflect on brightness variation and brightness difference, inasmuch as the shadow lies inside the invisible part of the crater. This explains also the entire subsequent course of brightness difference in Fig.11, $\sigma$ . In the case  $\partial$  (Fig.12, ) the shadow enters the invisible part earlier, and before angle  $i$  reaches its critical value. This is why the inflection of the function prior to fullmoon is shifted toward the side of larger values of angle  $i$ , and the brightness difference prior to fullmoon is systematically greater for the same values of  $i$  than after fullmoon for the same cause. The inflexion of the branch of the curve corresponding to the course of brightness variation after fullmoon, takes place at computed values of  $i_{cr}$ , for the shadow appears from the west. Because of the closeness of the areas near the lunar equator in the cases under consideration one may neglect the influence of azimuth variation. On the remaining curves of Fig.11 this influence is manifest to a substantially greater degree, but the general regularities are maintained.

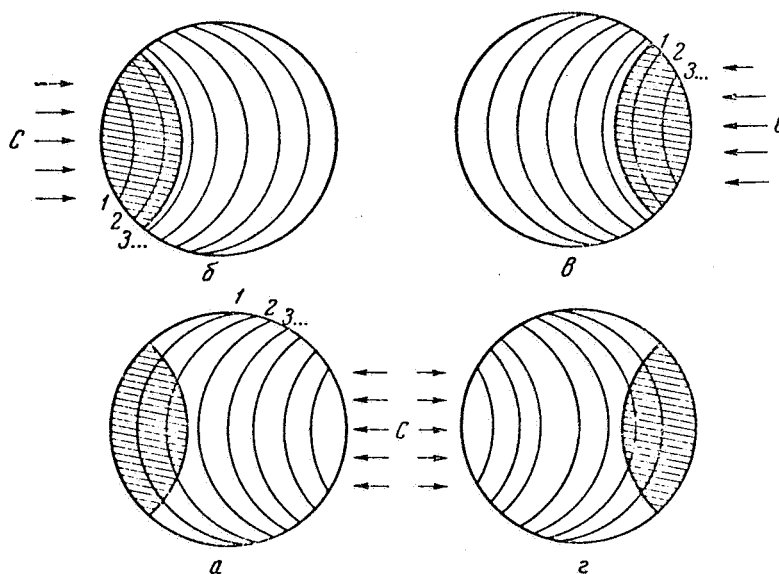


Fig.12. Sketch showing the disposition of the invisible region and of the shadow of the eastern (a, b) and western (c, d) craterlets. The arrows indicate the direction of solar rays and the numerals point to the sequence of shadow's motion

Finally, we shall pause at the case when azimuth varies most substantially, while the incidence and reflection angles' variations are negligibly small.

The curves of brightness variation for the radial system of the Numerov crater are plotted in Figure 13. Except for the case e, all curves show a sharp variation of the difference for an azimuth value of about  $50^\circ$ . It is noteworthy that for the case e, the incidence angle  $i = 35^\circ$ , i.e. it does not reach the critical value. For all the remaining points angle  $i$  exceeds the critical value and shadow must be present inside the craterlet.

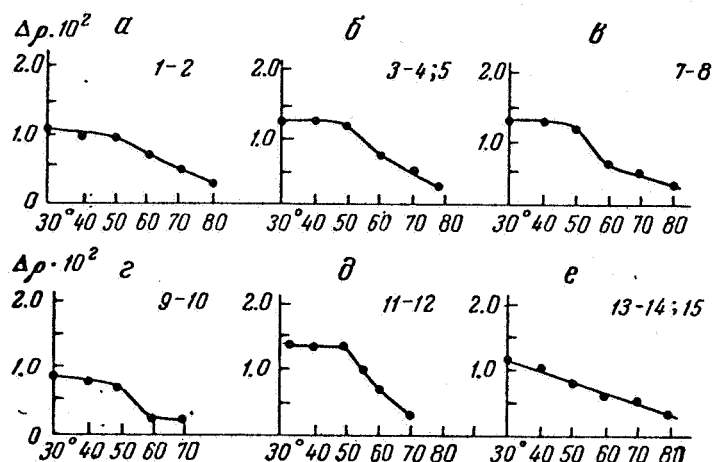


Fig.13. Curves of difference variation in the brightness of the ray and of comparison areas for the system of crater Numerov

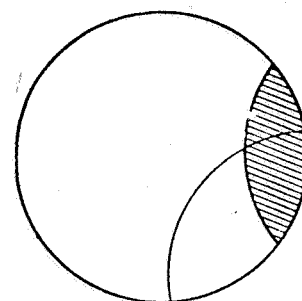


Fig.14. Sketch showing the disposition of the invisible region and shadow for an azimuth of about  $50^\circ$  and the case 13, a

Fig.14 shows a sketch of the disposition of the shadow and of the invisible part of the craterlet for the case 13, a and for an azimuth value of about  $50^\circ$  (when more than 50 percent of the shadow becomes visible). For lower values of the azimuth the shadow is visible only to a small degree. We may quite justifiably assume that the curves' steepness variation means that as the indicated value of azimuth is attained, the brightness variation of the craterlet at the expense of mesoshadow function begins to prevail over the variation on account of the change of angular parameters. The brightness of an element of ray drops and approaches that of the comparison area.

The interpretation developed here shows that the adopted structural model of light rays corresponds to the observed peculiarities of this morphological class of lunar formations.

\*\*\* T H E E N D \*\*\*

State Astronomical Institute  
of P. K. Shternberg  
(GAISH)

Manuscript received on  
8 July 1967

Contract No. NAS-5-12487  
VOLT TECHNICAL CORPORATION  
1145 - 19th St. NW  
WASHINGTON D.C. 20036

Translated by ANDRE L. BRICHANT  
on 2 - 5 June 1968

# R E F E R E N C E S

1. SHARNOV, V.V., Nature of Planet, M., Fizmatgiz, 1958.
2. SYTINSKAYA, N.N., Nature of Moon, M., Fizmatgiz, 1959.
3. ----- Technical report No.32-700 Ranger VII  
part II. Experimenters analyses and  
interpretations, JPL, Pasadena, California  
1965.
4. BUDBURY, P.V., Astronomical contribution from the Uni-  
versity of Manchester, series III, No.137.
5. FEDORETS, V.A., Trudy astronomicheskoy observatorii,  
KH.U.G. 2, 49, 1952.
6. HACKMAN, R.L., Lunar Rays, Geological Survey, Washington  
1961.
7. LIPSKIY, YU.N., PSKOVSKIY, YU.P., GURSHTEYN, A.A.,  
SHEVCHENKO, V.V., POSPERGELIS, M.M.,  
Outerspace Investigations, 4, vyp.6, 912,  
1966.
8. ----- "Atlas of the Far Side of the Moon" part II  
M., "NAUKA", 1976.
9. RADLOVA, L.N., Astronomicheskiiy zhurnal, 37, 1053, (1960).
10. BARABASHEV, N.P., CHEKIRDA A.G.,  
Tsirkulyar astronomicheskoy observatorii,  
KH.U.G., No.13, 3, 1955
11. CRONIN, J.F., ADAMS, J.B., COLOVELL, R.N., TIFFT, W.G.,  
Post Apollo Space Exploration, Part I,  
Washington, D.C., Amer. Astronaut. Soc.,  
435, 1966.
12. WHITAKER, E.A., The Nature of the Lunar Surface: proceedings  
of the 1965 IAU-NASA Symposium, 1966.
13. DIGGELEN, J. van Rech. astron. Observ. Utrecht, 14, 2,  
1958-1959.
14. BARABASHEV, N.P.,  
Investigation of Physical Conditions on the  
Moon and Planets, Izd-vo KH.U.G., KH. 1952.
15. KHABAKOV, A.V., On the Fundamental Questions of the History  
of Lunar Surface development. M., Geograf-  
giz., 1949.
16. ROSENBERG, D.L., Trans. Amer. Geophys. Union, 47, No.3, 486,  
1966.
17. MAKSUTOV, D.D., Astron. Optika, M. - L., Gostekhisdat, 1946.
18. SYTINSKAYA, N.N.,  
Astronomicheskiiy Zhurnal, 30, 3., 295, 1953.
19. KUIPER, G., Lunar Photographic Atlas, ed. by (G.Kuiper)  
Chicago, 1960.

\* \* \* \* \*